

# Electrochemical Deposition of $\gamma$ -Phase Zinc-Nickel Alloys from Alkaline Solution

Heidi A. Conrad, John R. Corbett, and Teresa D. Golden

Department of Chemistry, University of North Texas, Denton, Texas 76203, USA

Zinc-nickel alloys with 8-15% nickel were deposited onto stainless steel for corrosion protection. Alkaline deposition conditions were utilized given that alkaline systems have been found to offer superior substrate coverage which results in better corrosion protection of the metal substrate (stainless steel) compared to acid bath depositions. This method utilizes ammonium hydroxide as the base source with a working pH range of 9-9.5. Sodium acetate was used as the complexing ligand as it was found to stabilize the metal ions in the electrolytic solution. Strongly adhering, quality deposits were obtained with electrodeposition at room temperature. Bath compositions and applied potential had an effect on morphology of the films as seen in scanning electron microscopy. Upon examination by x-ray diffraction and atomic absorption spectroscopy, all deposits were confirmed as  $\gamma$  phase zinc-nickel alloys with a nickel content of 8-15%. The corrosion potential for the  $\gamma$ -phase coatings was improved over the pure zinc coatings.

## Introduction

In the field of corrosion resistance, there is a constant demand for increased performance at a reduced cost. Stainless steel is a common frame used in automobiles, planes, boats, and ships. In the regular use of these vehicles, stainless steel can be exposed to salt from the roads, from de-icing a plane, from salt water and more leading to corrosion problems. To lengthen the lifetime of these vehicles, the stainless steel can be coated with a metallic film that will corrode preferentially, thereby protecting the underlying stainless steel (1).

Zinc metal has been examined as a protective coating on stainless steel because the zinc coating is able to sacrificially corrode, which protects the underlying stainless steel substrate (2). Although zinc coatings were able to protect the underlying substrate, dissolution occurs fairly quickly during corrosion, so zinc alloys were examined as possible corrosion protective coatings.

The electrodeposition of metallic alloys is of great interest because the mechanical and chemical properties of the metals involved can be increased when alloyed (3). Originally zinc was alloyed with cadmium, but due to the harsh environmental conditions associated with cadmium, other metals were examined (4,5). Zinc-nickel alloys were examined as a replacement since nickel is cheap, easy to work with and the alloys offer comparable, if not better corrosion resistance than zinc-cadmium alloys (2). Zinc/nickel alloys have shown greater corrosion resistance than pure zinc coatings, and as the nickel content in the alloy increases, the corrosion potential increases (2). If the nickel content in the deposit becomes too great, the coating is a good barrier but once scratched or damaged will no longer protect the substrate.

There are 5 known phases for zinc-nickel alloys,  $\eta$ - (1% Ni),  $\alpha$  and  $\beta$ - (30% Ni, known as the nickel rich phases),  $\delta$ - ( $\text{Ni}_3\text{Zn}_{22}$ ) and  $\gamma$ - ( $\text{Ni}_5\text{Zn}_{21}$ ) known as the zinc rich phases (6,7,8). For maximum corrosion protection, the  $\gamma$  phase alloy tends to work best. The  $\gamma$  phase alloy offers the best corrosion resistance, with the nickel content between 8-15%, so this alloy phase is being extensively studied (6). In acidic baths  $\gamma$  phase deposition is observed along with  $\delta$  phase contamination.

The advantage of alkaline deposition for Zn-Ni is the deposit has a superior alloy distribution compared to acidic deposition; however the deposits tend to be duller in color, not the bright finishes obtained from acid baths (1). Alkaline electrodeposition gives a more uniform deposit, which offers better corrosion protection to the underlying metal. However, in alkaline baths, the zinc and nickel species must be stabilized with a complexing agent to prevent precipitation as metal hydroxides. Historically triethanolamine has been used as a complexing agent at pH ranges  $\geq 12$  (4).

This work focuses on electrodeposition of the  $\gamma$  phase zinc-nickel alloy under less caustic conditions. Deposition parameters such as pH, electrolyte composition, electrolyte concentration, and applied potential were studied for the deposition of the Zn-Ni alloys.

## Experimental

### Chemical Reagents and Methods

All solutions were prepared from reagent grade chemicals and deionized water with pH adjusted between 9 to 9.5 using  $\text{NH}_4\text{OH}$ . Zinc-nickel alloy layers were deposited from two plating bath solutions, A and B. Bath A consisted of  $\text{ZnSO}_4\cdot\text{H}_2\text{O}$ ,  $\text{NiSO}_4\cdot 6\text{H}_2\text{O}$  and sodium acetate and was deposited with a potential range of -1.00 to -1.40 V. Bath B consisted of  $\text{ZnSO}_4\cdot\text{H}_2\text{O}$ ,  $\text{Ni}(\text{NH}_4)_2(\text{SO}_4)_2\cdot 6\text{H}_2\text{O}$  and sodium acetate and was deposited with a potential range of -1.30 to -1.50 V. The ratio of zinc to nickel was controlled to obtain the correct alloy phase.

### Electrochemical Deposition

A simple three electrode cell was used for all depositions. The working electrode used throughout all electrochemical experiments was a stainless steel disc mounted in epoxy. The working electrode was polished with grit paper, diamond and alumina to obtain a mirror image on the surface of the electrode. The counter electrode used throughout all electrochemical experiments was a chromel coiled wire and the reference electrode was a saturated calomel electrode (SCE, +0.241 V vs. SHE). All deposits were obtained potentiostatically, both for the direct potential and potential step method. All electrochemical work was performed on an EG&G PAR Potentiostat/Galvanostat Model 273A.

### Analysis Techniques and Characterizations

All x-ray diffraction data was obtained on a Siemens D-500 Diffractometer using  $\text{Cu K}\alpha$  radiation ( $\lambda = 1.541 \text{ \AA}$ , 35 kV, 24 mA). The scans were run with a  $\theta$ : $2\theta$  coupled experiment, from  $35$ - $100^\circ$ , step size of 0.05 degrees and dwell time of 1 second.

The SEM micrographs were taken on an Environmental SEM, FEI Quanta 200 at an accelerating voltage of 25 kV using an ETD detector.

The zinc and nickel percentages in the films were measured with atomic absorption spectroscopy (AAS). A Perkin Elmer Analyst AAS Spectrophotometer was used, with hollow cathode lamps of zinc and nickel for the analysis.

The corrosion measurements for the coatings were obtained using linear polarization resistance measurements in a 0.1 M NaCl solution scanned to  $\pm 20$  mV from open circuit potential (OCP).

## **Results and Discussion**

### Deposition Bath Composition

Several nickel salt sources were examined as nickel ion sources for deposition. Typically nickel sulfate hexahydrate is used as a nickel source in Zn-Ni alloy depositions carried out in alkaline medium (4). Nickel sulfate hexahydrate readily dissolves in water, providing a source of nickel ions in an aqueous solution. Nickel ammonium sulfate hexahydrate was another salt examined as a possible nickel ion source. Nickel ammonium sulfate hexahydrate has not previously been examined for Zn-Ni deposition, but was studied due to the common ammonium ions with the base source used. While nickel ammonium sulfate hexahydrate is not as soluble in aqueous solutions as nickel sulfate hexahydrate, heating can be used to dissolve the compound. Once dissolved, the nickel ammonium sulfate hexahydrate can remain in solution for extended periods of time, even under alkaline conditions.

For zinc ion sources, zinc sulfate monohydrate was studied for the depositions. Zinc sulfate monohydrate does not dissolve as readily as other zinc sources that have been studied, but easily remains in solution once dissolved, even when exposed to more basic conditions and additional additives. Many other zinc sources require more intricate ligands and in this study a simplified approach was sought.

The pH of the solutions must be carefully controlled to obtain quality deposits. At varying pH ranges, you may obtain pure metal, or metal species such as metal hydroxides. Popov et. al. (9) observed that as the pH of the system was increased, the deposition potentials of the zinc and nickel species in solution were shifted to more negative values. The system can also absorb carbon dioxide from the air, thereby lowering the pH of the system, so fresh solutions must be used for the deposition. To adjust the pH, ammonium hydroxide was added to the solution. This base source was chosen because it negates the need for a buffer solution. The pH range of interest (9-9.5) was easily reached with ammonium hydroxide. The ammonia ions can also help stabilize the zinc and nickel species in solution, though not completely at this pH range, as a secondary complexing agent was required.

Sodium acetate was used alongside ammonia to aid in stabilizing the zinc and nickel ions in solution. Sodium acetate was chosen for the relatively simple structure and its ability to stabilize the zinc and nickel ions. However, the metal-ligand complex is not strong enough to prevent deposition. Nickel will readily precipitate out as a nickel hydroxide species under alkaline conditions, so complexing agents were required. The nickel ammonium sulfate hexahydrate remained in solution very well under alkaline conditions when using ammonium hydroxide as the base source so no added complexing ligand was required for this nickel ion source.

When Zn and Ni salts are combined for deposition, the metal ion species affect each others deposition potential. Anodic linear sweep voltammetry (ALSV) was used to determine the dissolution current of the species of interest. The effects of secondary

metals in solution were also examined. This method was used to obtain initial dissolution data of the zinc-nickel alloy of interest (10). The anodic linear sweep voltammograms in the presence of (a)  $Zn^{2+}$ , (b)  $Ni^{2+}$  and (c)  $Zn^{2+} + Ni^{2+}$  are shown in Figure 1 as a plot of the potential versus current. The potential was stepped from OCP to -1.5 V and held briefly before scanning back to OCP. Figure 1 shows the scan from -1.5 V to OCP. During this anodic scan stripping peaks were observed due to dissolution of the metals back into the electrolytic solution. From Figure 1, it is clear that zinc individually has a strong anodic dissolution peak present at -1.10 V. Nickel has a smaller anodic dissolution peak present at -0.48V. When combined in solution, the zinc and nickel anodic dissolution peaks are shifted from the original values. The alloy metal dissolution peaks lie between the potentials observed for individual  $Zn^{2+}$  and  $Ni^{2+}$  in solution. This data suggests that codeposition of the alloy allows zinc to deposit at more positive potentials and the nickel to deposit at more negative potentials. In the combined solution the zinc anodic stripping peak is present at -0.68 V and the nickel stripping peak is present at -0.54 V. The anodic dissolution potentials of the zinc and nickel metals have been shifted in the combined solution, showing the metals affect the deposition of one another when combined. The zinc-nickel alloy of interest undergoes anomalous deposition, so a dependence of the dissolution peaks of the metals relative to one another is expected.

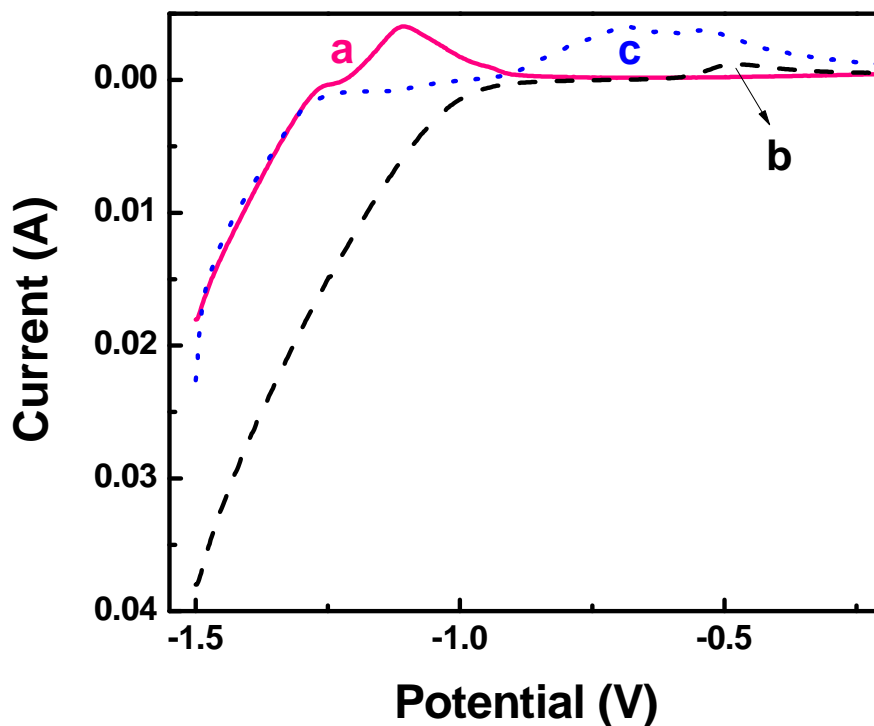


Figure 1. Linear sweep voltammogram of (a) zinc (solid line), (b) nickel (dash line), and (c) zinc-nickel alloy (dotted line).

Two different bath compositions were tested for deposition of the Zn-Ni films, Bath A and Bath B. Bath A was composed of the following components: zinc sulfate monohydrate, nickel sulfate hexahydrate, ammonium hydroxide and sodium acetate in an

aqueous medium. All deposits were run at room temperature, with a pH range of 9-9.5 using sodium acetate as a complexing ligand to stabilize both zinc and nickel ions in solution. Bath B was composed of the following components: zinc sulfate monohydrate, nickel ammonium sulfate hexahydrate, ammonium hydroxide and sodium acetate in an aqueous medium. All deposits were run at room temperature, with a pH range of 9-9.5 using sodium acetate as a complexing ligand to stabilize the zinc ions in solution. The nickel ammonium sulfate hexahydrate does not require an additional complexing ligand to remain in solution under alkaline conditions. Chronocoulometry (CC) was used to determine if the concentrations of the zinc or nickel species in solution must be controlled in the electrochemical bath to aid deposition of the  $\gamma$  phase alloy. The diffusion coefficients of zinc and nickel in alkaline solution with acetate ligand were determined to be  $1.13 \times 10^{-4}$  and  $2.86 \times 10^{-4}$  cm<sup>2</sup>/s, respectively.

Based on previous depositions and chronocoulometry experiments, it was known that the zinc and nickel molar ratios must be carefully controlled for deposition of the  $\gamma$  phase alloy to occur. A range of 2:1 to 4:1 molar ratio equivalent of Zn-Ni was examined for the electrochemical deposition bath. If the ratio of zinc to nickel is too high, the coating will be deposited as pure zinc based on the XRD results. Upon further examination of these deposits with AAS, it is observed there are small amounts of nickel present in the deposit (2-5%) but the amount is small enough as to not cause a transition to  $\gamma$  phase deposition. Zinc is hexagonal in structure, nickel is face centered cubic while  $\gamma$  phase is body centered cubic, and so a definite structural difference is observed for different percentages of zinc and nickel in an alloy. A higher amount of nickel in the bath would result in a pure nickel coating, so the concentration of the nickel sulfate hexahydrate was also controlled in the electrochemical bath. Nickel is able to diffuse to the electrode surface at a faster rate than zinc (which is diffusion limited), so the concentration must be controlled to obtain the  $\gamma$  phase alloy deposition.

#### Deposition conditions for Zn-Ni films

Both baths were tested using direct potential and potential step depositions for the optimal coatings of the alloys. Initial studies were performed with direct potential methods, but the coatings appeared uneven, flaky and were easily removed from the stainless steel surface. A potential step method was used to improve the coating deposition. The coatings were of much better quality, had a strong adhesion to the metal substrate, and gave more evenly distributed coating.

Potential step methods are also useful to aid in the release of hydrogen gas that can become trapped in the deposit due to the high overpotentials used for deposition. Trapped hydrogen often leads to hydrogen embrittlement, which can deteriorate the coating at a faster rate and cause problems in the corrosion coatings composed of a zinc-nickel alloy. The microstructures of the deposits determine how hydrogen will affect the deposit. Small microcracks in the deposit can release the hydrogen without damaging the coating, and without leading to further corrosion. Uniformly disturbed microcracks can minimize the attack of corrosion cells through the method of microcracking. More open grained structures are also preferred since hydrogen can easily escape these coatings, without damaging the overall structure (10-12). At the high potentials required for  $\gamma$  phase alloy deposition, hydrogen evolution can easily become a side product, so potential step techniques help with the release of any hydrogen in the deposits. In addition, pulse plating increases the nucleation rate resulting in finer grain coatings (13).

## Characterization of the electrodeposited Zn-Ni coatings

The cyclic voltammogram (CV) of Bath A is presented in Figure 2. Peak (a) is due to zinc dissolution and peak (b) is due to nickel dissolution. According to Lin et. al. (14), the wide separation of the zinc and nickel dissolution peaks can support alloy deposition when utilizing a potential step method. Based on the CV in Figure 2, the depositions were performed with a potential step method, with the potential ranging from -1.0 to -1.4 V, with a longer delay at the elevated potential. The potential step method allows both zinc and nickel ions to deposit onto the metal substrate at higher overvoltages and remove some of the film at lower voltages. When the potential is stepped between the two potentials it creates a better adhering, stronger, more uniform deposit, which results in better corrosion protection. After deposition, the coatings were characterized by several techniques.

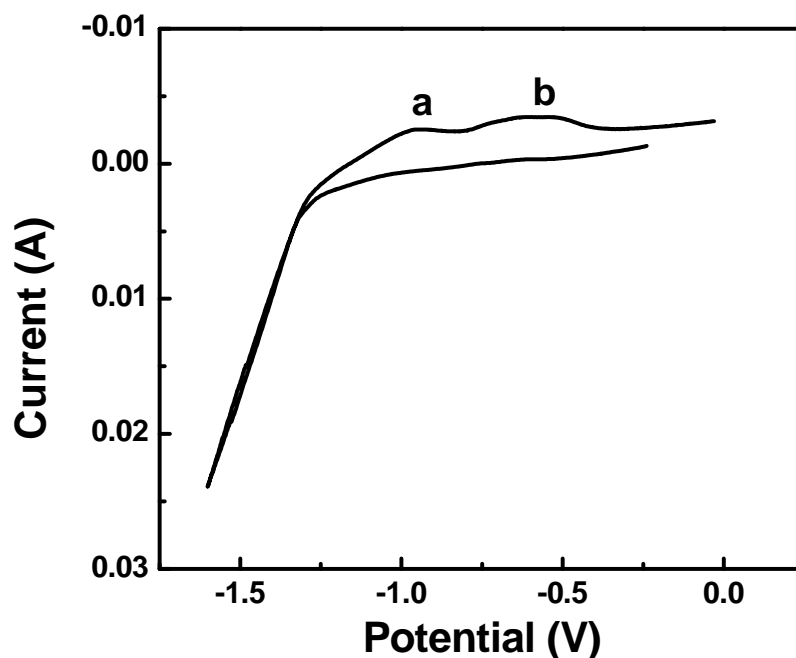


Figure 2. Cyclic voltammogram of 3:1 molar ratio of  $\text{ZnSO}_4 \cdot \text{H}_2\text{O}$ :  $\text{NiSO}_4 \cdot 6\text{H}_2\text{O}$  solution at pH 9.37 adjusted with 1 M  $\text{NH}_4\text{OH}$ , (a) zinc stripping peak, (b) nickel stripping peak.

The zinc-nickel alloy of interest has a body centered cubic (bcc) lattice structure and has a chemical formula of  $\text{Ni}_5\text{Zn}_{21}$ . The XRD pattern (Figure 3) confirms the presence of  $\gamma$  phase Zn-Ni preferentially deposited onto the substrate. There is a (330) reflection for the  $\gamma$  phase present in the pattern (per pdf #06-0653 JCPDS Database). All the other peak assignments belong to the substrate. In many methods,  $\delta$  phase contamination is present in the deposits, as this phase is readily deposited at similar potentials. The  $\delta$  phase is an impurity; the deposit exhibits the best corrosion protection when pure  $\gamma$  phase is only present (11). This XRD pattern confirms the sole presence of  $\gamma$  phase alloy, which is ideal for corrosion protection. However the (330) reflection is weak since the deposit thickness is thin. Zn-Ni  $\gamma$  phase alloys were also analyzed with AAS and the deposits were within the range for  $\gamma$  phase for maximized corrosion protection (8-15% Nickel).

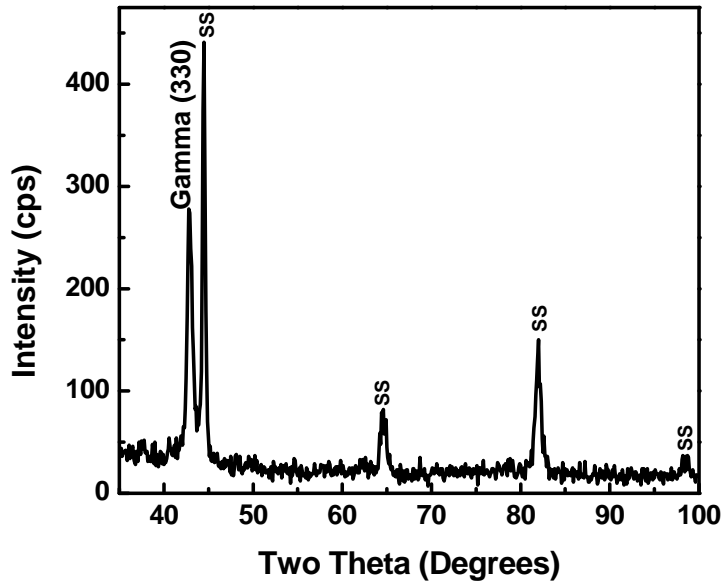


Figure 3. X-ray diffraction pattern of  $\gamma$  phase Zinc-Nickel alloy coating deposited from a 3:1 molar ratio of  $\text{ZnSO}_4 \cdot \text{H}_2\text{O}$ :  $\text{NiSO}_4 \cdot 6\text{H}_2\text{O}$  solution at pH 9.37.

The morphological characteristics of the Zn-Ni alloys utilizing Bath A parameters were also examined with SEM. The coatings were not uniform across the surface and contained many voids. Figure 4a was deposited from a solution of 3:1 ratio of zinc to nickel with acetate in the electrochemical bath. Even changing the Zn-Ni ratio did not completely improve the uniformity across the surface. At a 4:1 ratio of zinc to nickel, there were still voids across the surface of the film (Figure 4b). A second nickel source for Bath B was then tested to obtain better coatings.

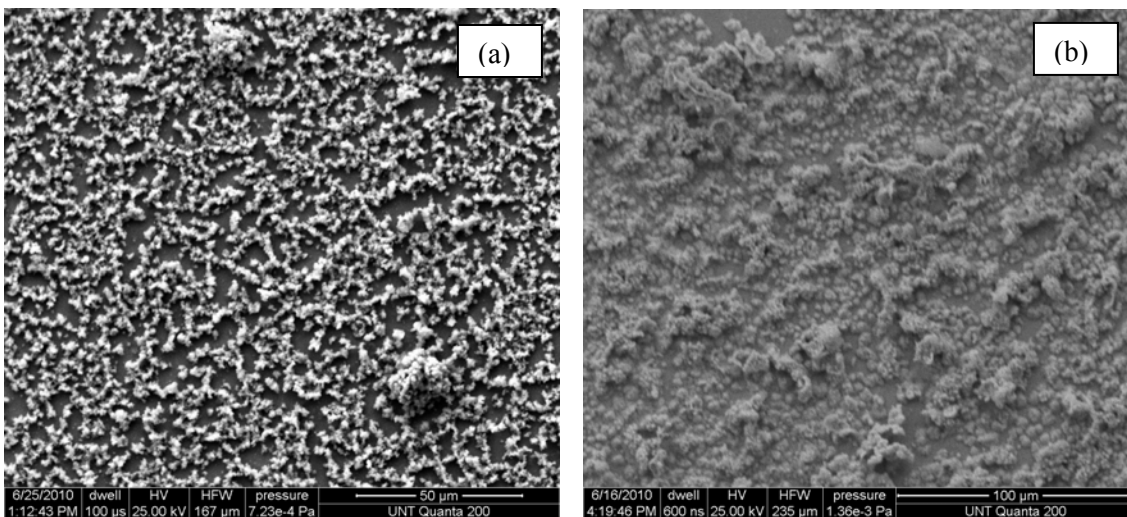


Figure 4. Scanning electron micrograph of Zn-Ni alloy coating on stainless steel deposited from a (a) 3:1  $\text{ZnSO}_4 \cdot \text{H}_2\text{O}$ :  $\text{NiSO}_4 \cdot 6\text{H}_2\text{O}$  ratio solution at pH 9.37 and a (b) Zn-Ni alloy film deposited on stainless steel from a 4:1  $\text{ZnSO}_4 \cdot \text{H}_2\text{O}$ :  $\text{NiSO}_4 \cdot 6\text{H}_2\text{O}$  ratio solution at pH 9.37 adjusted with 1M  $\text{NH}_4\text{OH}$ .

The cyclic voltammogram (CV) of Bath B is presented in Figure 5. Peak (a) is due to zinc dissolution and peak (b) is due to nickel dissolution. There is a crossover in the CV at (c). A crossover represents where nucleation of the metals onto the substrate begins to occur. So to obtain a deposit, one needs to consider not only the dissolution peaks of the two metals of interest, but also the crossover point where nucleation has begun. Based on the CV in Figure 5, the depositions were performed with a potential step method, with the potentials ranging from -1.0 to -1.4 V and from -1.3 to -1.5 V, with longer delay at the elevated potential. Strong adhering metallic films were present on the electrode after deposition and characterized with several techniques.

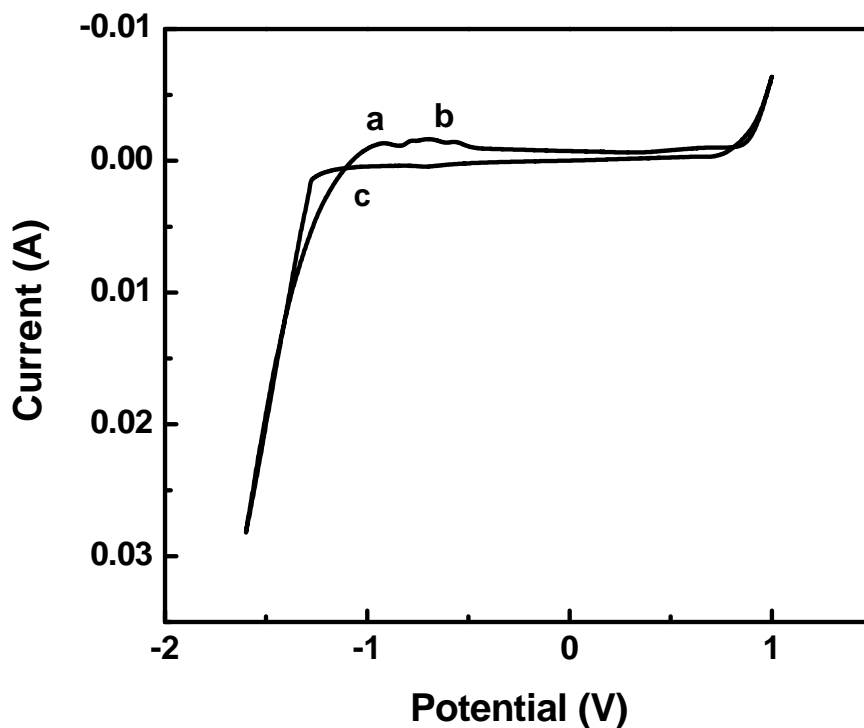


Figure 5. Cyclic voltammogram of 2:1  $\text{ZnSO}_4 \cdot \text{H}_2\text{O}$ :  $\text{Ni}(\text{NH}_4)_2(\text{SO}_4)_2 \cdot 6\text{H}_2\text{O}$  solution at pH 9.36 adjusted with 1M  $\text{NH}_4\text{OH}$ . (a) zinc stripping peak, (b) nickel stripping peak, (c) crossover.

The  $\gamma$  phase Zn-Ni alloy structure was again confirmed with XRD. It is clear from Figure 6, that gamma phase was preferentially deposited showing a strong (330) reflection (confirmed by PDF#06-0653 JCPDS Database). As with the results for Bath A, all coatings deposited under Bath B conditions exhibited preferential deposition for the  $\gamma$  phase. However, the deposition from Bath B shows a much stronger (330) reflection than Bath A pointing to a much thicker coating. No other phases, such as  $\delta$  phase were present, which is a common contaminant in  $\gamma$  phase deposition. The zinc and nickel content of the deposits which were confirmed as  $\gamma$  phase zinc-nickel alloy were analyzed with AAS and the deposits were within the range of interest for maximized corrosion protection (8-15% nickel).

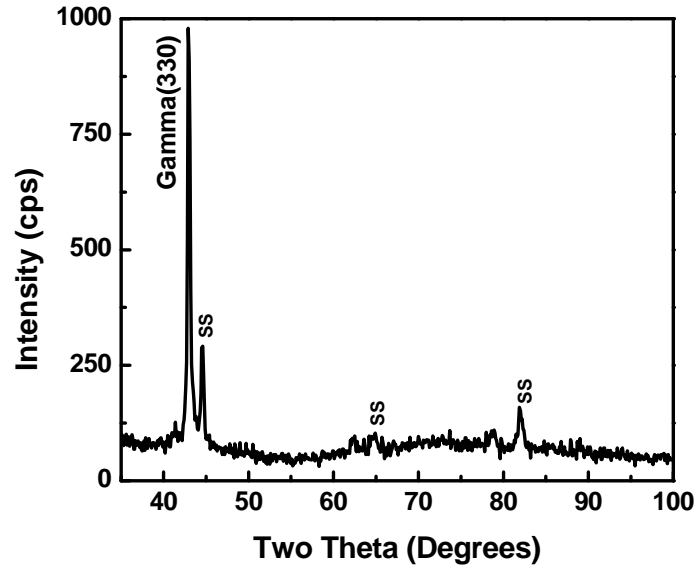


Figure 6. XRD pattern of Zn-Ni alloy film deposited from a 2:1  $\text{ZnSO}_4 \cdot \text{H}_2\text{O} : \text{Ni}(\text{NH}_4)_2(\text{SO}_4)_2 \cdot 6\text{H}_2\text{O}$  solution at pH 9.36 adjusted with 1M  $\text{NH}_4\text{OH}$ .

The morphological characteristics of the deposits were analyzed with SEM. Figure 7a shows the SEM of the 2:1 ratio of zinc to nickel in the bath. This bath results in a much more uniform deposition surface, but still contains voids and cracks on the surface. Zn-Ni coatings with more compacted spherical grains exhibit better corrosion protection than other morphologies (4).

A second deposit with the same ratio of metals was examined but was deposited at a higher overpotential. This deposit exhibits more uniform grain size as shown in Figure 7b, which is preferred for corrosion protection. It is clear Bath B leads to a better coverage and coating on the electrode surface. The grain sizes present for the second Bath B deposit are also more uniform, which results in increased corrosion protection.

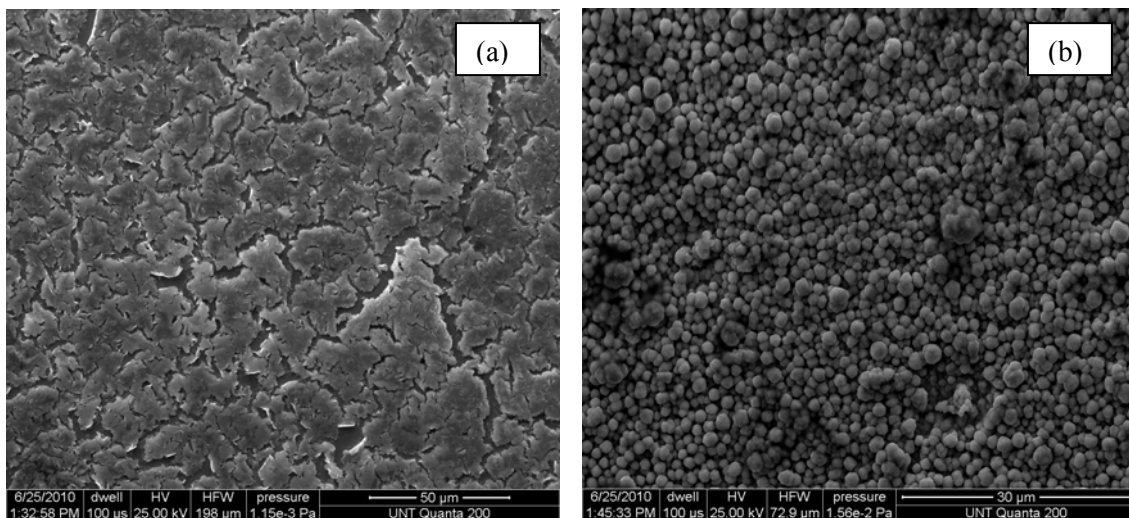


Figure 7. Scanning electron micrographs of Zn-Ni film deposited from Bath B at (a) low overpotential and (b) at high overpotential.

Corrosion studies were done for pure Zn, pure Ni and Zn-Ni  $\gamma$  phase for coatings from Bath A and B. The corrosion potential ( $E_{\text{corr}}$ ) of the various coatings are given in Table 1. The data shows a decrease in  $E_{\text{corr}}$  for the  $\gamma$  Zn-Ni coatings over pure Zn giving an increase in corrosion resistance for the alloy coatings. The corrosion current also decreased in the alloy compared to pure zinc. The anodic peak of the alloy again lies at a more positive potential relative to pure zinc, but relative to the Ni film formed with  $\text{NiSO}_4 \cdot 6\text{H}_2\text{O}$  at a more negative potential. This alloy retains properties more similar to pure zinc, but still incorporates nickel, which increases the corrosion resistance of the deposit. The corrosion current also decreased in the alloy compared to pure zinc.

**TABLE I.** Corrosion current and potentials vs. SCE in 0.1M NaCl solution.

<b>Deposit</b>	<b><math>I_{\text{corr}}</math> (mA)</b>	<b><math>E_{\text{corr}}</math> (V)</b>
Zn only	3.14E-4	-1.141
Ni only (Bath A)	1.07E-5	-0.344
Ni only (Bath B)	1.09E-4	-0.580
Zn-Ni $\gamma$ -phase (Bath A)	1.85E-5	-0.822
Zn-Ni $\gamma$ -phase (Bath B)	4.36E-5	-0.979

## Conclusions

Bath A and Bath B resulted in pure  $\gamma$  phase zinc-nickel alloy deposition confirmed by XRD, all coatings preferentially deposited to the  $\gamma$  phase with a preferred (330) orientation. When analyzed with AAS, the nickel concentrations from all deposits were within the nickel range of interest (8-15% nickel). Bath B results in a better covering, more uniform grain size deposit, compared to Bath A. Based on these results, Bath B would provide optimal corrosion protection, being able to better withstand corrosion cell formation for a longer time frame.

Zinc sulfate monohydrate has been used throughout all depositions and is a good zinc source for  $\gamma$ -phase alloy deposition. Nickel sulfate hexahydrate and nickel ammonium sulfate hexahydrate were examined as nickel ion sources for deposition, but nickel ammonium sulfate hexahydrate exhibited better morphology when alloyed with zinc compared to coatings obtained with nickel sulfate hexahydrate. Bath A and Bath B both exhibited nickel percentages in the range of interest (8-15% nickel) so the main distinction is based on the SEM data showing a more even coating present when deposited under Bath B conditions. The molar ratios of zinc and nickel must be carefully controlled in the electrochemical bath to obtain pure  $\gamma$  phase zinc nickel alloy.

Zinc-nickel alloy deposition requires a large overpotential to deposit onto the stainless steel electrode. At lower current densities, other alloy phases are formed but to obtain pure  $\gamma$  phase alloy, a high overpotential is required. At this high overpotential, the kinetic barriers of nickel are overcome but the diffusional barriers of zinc have not been compensated for so careful control of concentration ratios in the solution must be maintained.

The potential step method proved better for both Bath A and Bath B depositions. Stronger adhering films were obtained when deposited from the step potential method than from direct deposition. With this method we are able to obtain smoother deposits in an equivalent time frame, making this method desirable for the wider scope of applications.

## Acknowledgments

The authors gratefully acknowledge the Center for Advanced Research and Technology (CART) at the University of North Texas for access to the SEM experimental facilities used for this study. The authors thank Thanh D. Nguyen for obtaining the SEM results and photos.

## References

1. P.C. Wynn, in Proceedings- *AESF SUR/FIN* 510 (2001).
2. N. Zaki, *Metal Finishing.*, **6**, 57 (1989).
3. M.M. Abou-Krishna, *Applied Surface Science*, **252**, 1035 (2005).
4. H.Y. Lee and S. G. Kim, *Surface and Coatings Technology*, **135**, 69 (2000).
5. P. Ganesan, S.P. Kumaraguru and B.N. Popov, *Surface and Coatings Technology*, **201**, 3658 (2006).
6. J.B. Bajat, M.D. Maksimovic, V. B. Miskovic-Stankovic and S. Zec, *Journal of Applied Electrochemistry*, **31**, 355 (2001).
7. A. Petrauskas, L. Grinceviciene, A. Cesuniene and E. Matulionis, *Surface and Coatings Technology*, **192**, 299 (2005).
8. C. Muller, M. Sarret and M. Benballa, *Electrochimica Acta*, **46**, 2811 (2001).
9. H. Kim, B. N. Popov and K. S. Chen, K. S., *Journal of the Electrochemical Society* **150**, C81 (2003).
10. Y.F. Jiang Et Al, *Thin Solid Films*, **484**, 232 (2005).
11. M.S. Michael and S. Radhakrishna, *Anti-Corrosion Methods and Materials*, **45**, 113 (1998).
12. J. A. Bates, *Plating and Surface Finishing*, **81**, 36 (1994).
13. P. Ganesan, S.P. Kumaraguru and B.N. Popov, *AESF SUR/FIN*, 1064 (2004).
14. Y.P. Lin and J. R. Selman, *Journal of the Electrochemical Society*, **140**, 1229 (1993).